

Route to a chaotic state in fluid flow past an inclined flat plate

Jie Zhang, Nan-Sheng Liu, and Xi-Yun Lu*

Department of Modern Mechanics, University of Science and Technology of China, Anhui, Hefei 230026, China

(Received 29 October 2008; published 27 April 2009)

We present the results of a numerical study of flow past an inclined flat plate and reveal a route of the transition from steady to chaotic flow. We find that the chaotic flow regime can be reached through the sequential occurrence of successive period-doubling bifurcations and various incommensurate bifurcations. The results provide physical insight into the understanding of fundamental flow behaviors underlying in this flow system and complement the transition phenomenon from steady to chaotic flow.

DOI: [10.1103/PhysRevE.79.045306](https://doi.org/10.1103/PhysRevE.79.045306)

PACS number(s): 47.20.Ky, 47.11.Qr, 47.15.Fe, 47.52.+j

Transition from a laminar to chaotic flow through diverse routes is of significance in fundamentals and applications. In the general theory of nonlinear dynamics, the dynamical system may become chaotic via period-doubling bifurcations (Feigenbaum scenario [1,2]), various incommensurate bifurcations (Ruelle-Takens-Newhouse scenario [3,4]), or intermittency regime (Manneville and Pomeau scenario [5]). Based on previous studies in closed and open flows, such as Rayleigh-Bénard convection, Taylor-Couette flow, and binary mixture convection, we have noticed that the transitional routes of these flows to chaotic states may solely take the period-doubling bifurcations [6,7] or the various incommensurate bifurcations [8–10].

Flow of a fluid past a body, e.g., cylinder and flat plate, is a well-known phenomenon in daily life and engineering, and involves complicated flow dynamics. A most important parameter to characterize this kind of flow is the Reynolds number (Re) [11]. When Re is over a critical value in the flow past a cylinder or an inclined flat plate, the transition from steady to periodic flow marked by a Hopf bifurcation was exhibited [11]. As Re increases further, the flow behind a circular cylinder transforms to chaos following the period-doubling bifurcations [12]. However, the transition route from steady to chaotic state for flow past an inclined flat plate has never been studied but is highly desirable for understanding the fundamental flow behaviors. Here we show this transition route and reveal a transition process with both the period-doubling and various incommensurate scenarios occurring sequentially.

We consider the flow system as an incompressible fluid with free-stream speed U past an inclined flat plate of length L shown in Fig. 1. Two control parameters are the inclined angle α with respect to the free-stream flow and the Reynolds number $Re=UL/\nu$ with ν as the kinematic viscosity of the fluid. Here, a systematical study was carried out for $0 \leq \alpha \leq 45^\circ$ and $Re \leq 800$. The methodology is a direct numerical simulation using a multiblock lattice Boltzmann method [13,14] with second-order accurate treatment for the boundary conditions [15]. No-slip boundary condition is used on the body surface. Our code has been validated carefully [16,17]. Following our extensive tests, the computa-

tional domain is chosen as $-10 \leq x \leq 30L$ and $-10 \leq y \leq 10L$ with the finest lattice spacing $0.005L$ in the near region of the plate. To reliably identify the flow states, the computed time elapses to $3000L/U$.

We first summarize our findings in the $Re-\alpha$ plane for the transition route of the flow system from steady to chaotic state. When Re or α increases in Fig. 2(a), the flow from steady in region I to periodic state in region II occurs via a Hopf bifurcation. Figure 2(b) shows the basic frequency f_1 normalized by U/L , corresponding to the boundary of I and II [Fig. 2(a)]. The frequency f_1 decreases with the increase in α . As a validation, the present results shown in Figs. 2(a) and 2(b) agree well with previous data predicted by Jackson [11] who only dealt with the Hopf bifurcation. For subsequent motions in the periodic state in Fig. 2(a), the first period-doubling bifurcation is generated from regions II to III, where subharmonic frequency $f_1/2$ is excited via a spectral analysis shown below. Then, a sequence of successive period-doubling bifurcations is detected in region III.

Based on our fine numerical experiments, we have noticed that, unlike a usual transitional route of the period-doubling bifurcations in some flows [6,7], the present flow system does not enter chaotic state at the “end” of the period-doubling bifurcations. In Fig. 2(c) for an enlarged view of region III, two- and three-frequency quasiperiodic flow states are identified in the quasiperiodic region. The flow subsequently becomes chaotic state via the various incommensurate bifurcations, similar to the Ruelle-Takens-Newhouse scenario. As an example, Fig. 2(d) shows the successive period-doubling and various incommensurate bifurcations leading to chaos as the increase in Re at $\alpha=25^\circ$. Here we find that the period-doubling and various incommensurate bifurcations coexist in a flow system.

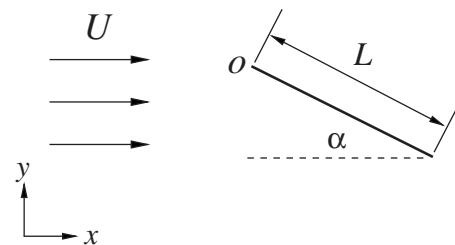


FIG. 1. Sketch of free-stream flow of a fluid past an inclined flat plate. Cartesian coordinate system (x,y) with the origin o at the leading edge of the plate is used.

*Author to whom correspondence should be addressed. FAX: +86-551-3606459. xlu@ustc.edu.cn

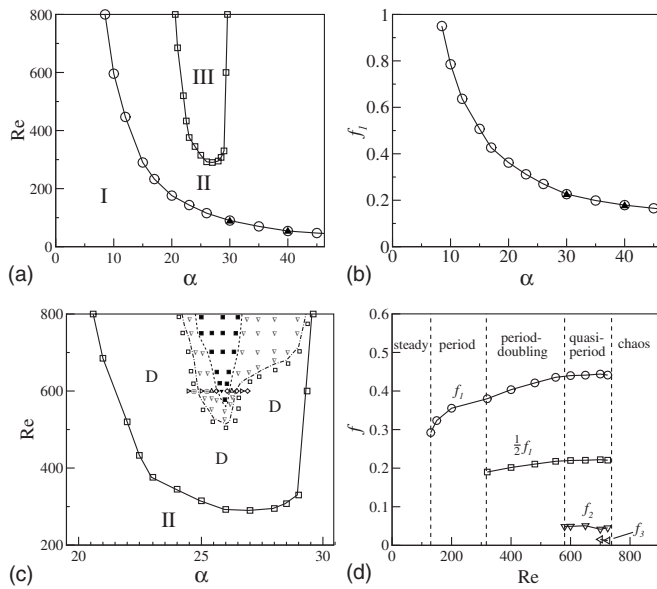


FIG. 2. Sketches of the transition from steady to chaotic flow. (a) Boundaries of critical parameters for the Hopf bifurcation plotted by the line plus \circ and the first period-doubling bifurcation by the line plus \square . I represents steady-state region, II one frequency-locking region, and III complicated region. \blacktriangle represents the data in [11]. (b) The basic frequency f_1 corresponding to the boundary between I and II. \blacktriangle is the data in [11]. (c) Enlarged view of region III. D represents the period-doubling region. The region marked by symbols is a fine calculation zone with dense selected parameters Re and α . These symbols represent period-doubling regime (\square), quasiperiodic regime (∇), and chaotic regime (\blacksquare). Flow past an elliptic airfoil at $Re=600$ exhibits periodic (\oplus) and period-doubling state (\diamond) at $\lambda=0.3$, and period-doubling (\triangleright), quasiperiodic (\triangle), and chaotic state (\blacktriangledown) at $\lambda=0.1$. (d) Schematics of the successive bifurcations leading to chaos versus Re at $\alpha=25^\circ$.

According to the overview of the flow states in the Re - α plane, we then discuss the relevant behaviors in detail using Fourier power spectra, vortical structures, and phase-space trajectories. To clearly present the results in Figs. 2(a) and 2(c), we will exhibit the transition processes from steady to chaotic flow via a fixed $\alpha=25^\circ$ varying with Re and via a fixed $Re=600$ varying with α , respectively.

Figure 3 shows the Fourier power spectra of the velocity at point $x=L$ and $y=-0.45L$ for $\alpha=25^\circ$, corresponding to Fig. 2(d). The power spectrum contains a series of peaks at the primary frequency f_1 and its harmonic frequencies $2f_1$, $3f_1$, etc. for $Re=315$ [Fig. 3(a)]. The flow system is a frequency-locking phenomenon. To understand the bifurcation behaviors, the corresponding vortical structures in the physical space are shown in Fig. 4. It is seen that regular von Kármán vortex street is formed in the wake for $Re=315$ [Fig. 4(a)]. As Re increases to 320, subharmonic frequency $f_1/2$ is excited in Fig. 3(b). We have identified that the transitional process via the period-doubling bifurcation exists up to $Re=575$. The occurrence of a period-doubling can be explained as follows. In the development of vortices in the wake [Fig. 4(b)], the vortices have the trend of pairing over twice primary periods $2T_1$ with $T_1=1/f_1$, consistent with the findings of flow past a circular cylinder [12]. It is worth mentioning

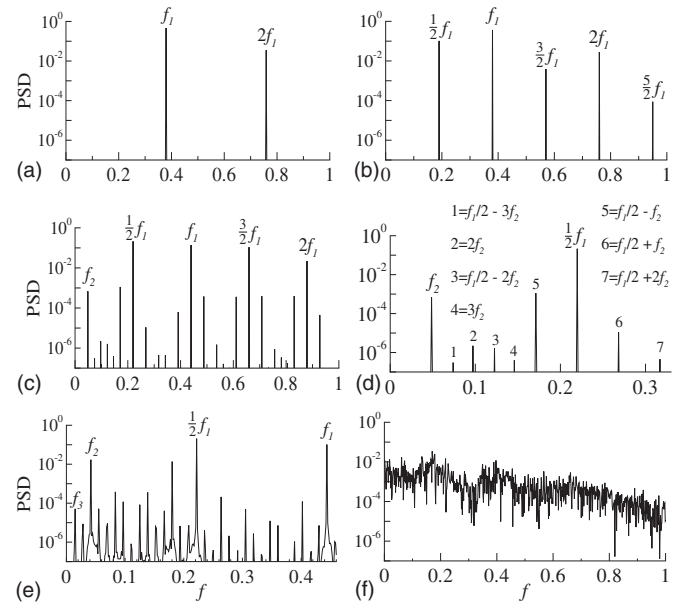


FIG. 3. Power spectrum density (PSD) of the velocity component in the y direction at point $x=L$ and $y=-0.45L$ for $\alpha=25^\circ$ and (a) $Re=315$, (b) 320, (c) and (d) 580, (e) 700, and (f) 800. Here, (d) is an enlarged view of (c).

that the period-doubling bifurcation does not lead to vortex merging and the wake retains its basic spatial structure [12]. In contrast, the appearance of a subharmonic phenomenon in shear layer flow does imply vortex merging [18].

With the increase of Re , two- and three-frequency quasi-periodic flow states are generated. For $Re=580$ [Fig. 3(c)], the second basic frequency f_2 is excited in the power spectrum, where the winding number, $W=f_2/f_1$ [19], is irrational. Spectral peaks in Fig. 3(d) occur in linear combinations of the two frequencies related by $m_1(f_1/2)+m_2f_2$, with m_1 and m_2 as integers. Correspondingly, Fig. 4(c) shows the vortical pattern, similar to a well-organized vortical structure in the wake of an transversely oscillating circular cylinder [20], characterized by both lines of vortex-pairs moving downward due to their induced velocity and of vortices ranked by opposite signs alternately, resulting in f_2 in the vortices evolution. With the increase in Re , e.g., $Re=700$ [Fig. 3(e)], the third basic frequency f_3 is excited with the irrational winding

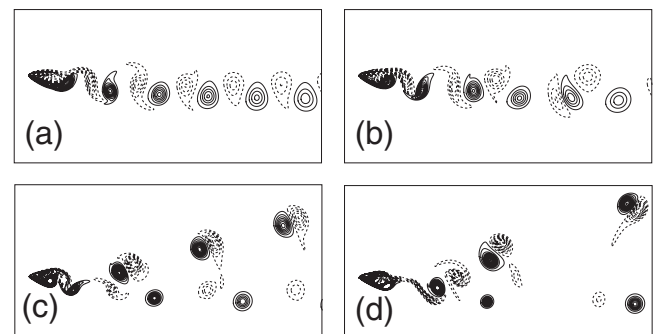


FIG. 4. Instantaneous vorticity contours at $\alpha=25^\circ$ and (a) $Re=315$, (b) 320, (c) 580, and (d) 800. Solid lines represent positive values and dashed lines negative values.

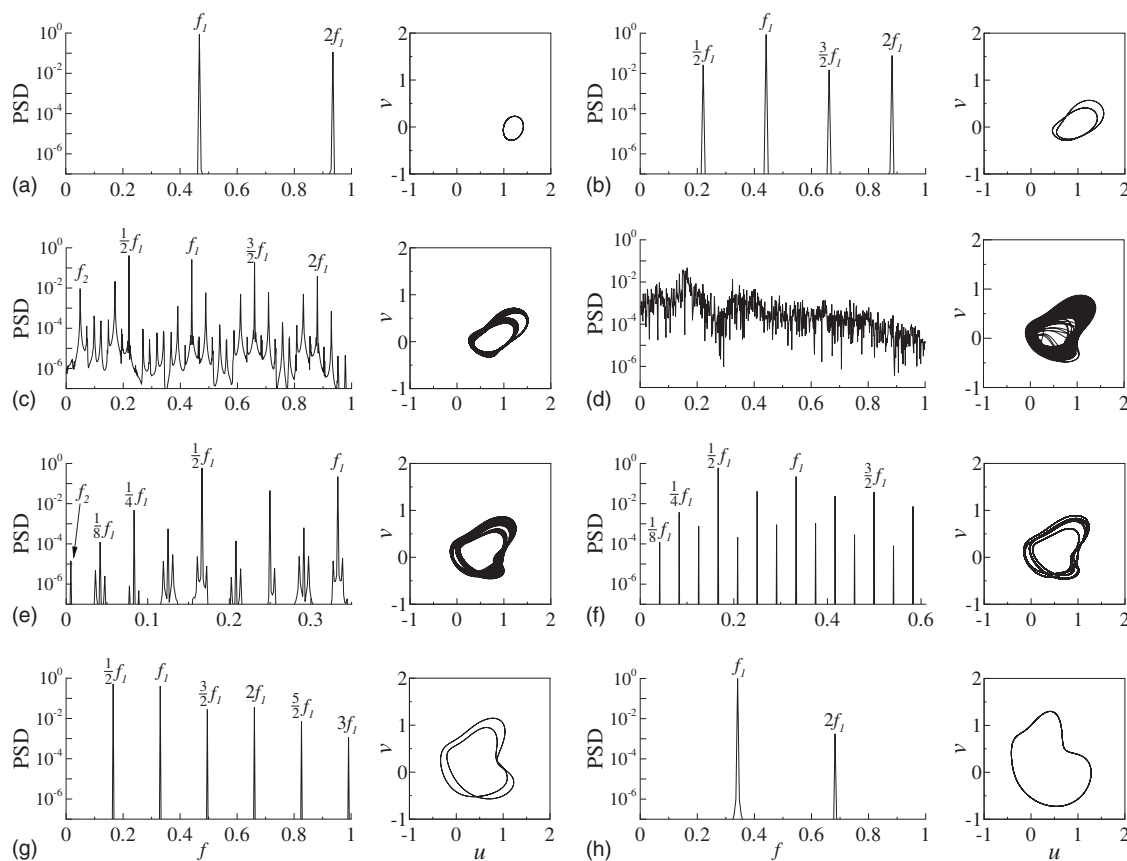


FIG. 5. Power spectrum density of the velocity and phase-space plot of the velocity components (u, v) at point $x=L$ and $y=-0.45L$ for $Re=600$ and (a) $\alpha=21$, (b) 24, (c) 25, (d) 26, (e) 26.3, (f) 26.5, (g) 28, and (h) 30° .

numbers f_2/f_1 and f_3/f_1 , and peaks in the power spectrum are related to the linear combinations of $f_1/2$, f_2 , and f_3 . From the above analysis, we can reasonably understand that the route of the transition from steady to chaotic flow is closely associated with the vortices evolution behind the plate.

When Re is further increased to 800, an aperiodic behavior occurs. The broadband continuous spectrum in Fig. 3(f) clearly depicts the chaotic behavior, and the vortex structure in Fig. 4(d) shows complex aperiodic interactions. The dynamical nature of the transition process from order to chaotic state may be diagnosed by calculating the largest Lyapunov exponent, λ_E [21], from the time-dependent data obtained numerically. Using the treatment [9], near zero values of the Lyapunov exponents are predicted for nonchaotic flows up to $Re=730$ approximately in Fig. 2(d). Positive Lyapunov exponents are obtained for $Re > 730$, e.g., $\lambda_E \approx 0.38$ for $Re = 800$, and verify chaotic flow character.

Further, we briefly describe the transition processes varying with α at a fixed Reynolds number $Re=600$. The power spectra and the phase-space plots of the velocity components (u, v) are shown in Fig. 5, respectively. At $\alpha=21^\circ$ [Fig. 5(a)], the flow lies in periodic region with a primary frequency f_1 in the power spectrum and one limit cycle in the phase-space. With the increase in α , a period-doubling bifurcation occurs at $\alpha=24^\circ$ [Fig. 5(b)], resulting in a peak of $f_1/2$ and branching into two connected limit cycles. When $\alpha=25^\circ$ [Fig. 5(c)], a second frequency f_2 is excited in the power

spectrum and spectral peaks occur in a relation of $m_1(f_1/2) + m_2f_2$. The corresponding phase-space exhibits two limit tori which depict the quasiperiodic behavior. Further, as α increases to 26° [Fig. 5(d)], the broadband continuous spectrum is generated and an extremely tangled plot clearly presents that the flow has resulted in a chaotic state, which is confirmed by $\lambda_E \approx 0.26$.

Following the above transition process, we have noticed that the flow state is sensitive to the change of α in the local region around $Re=600$ and $\alpha=26^\circ$ shown in Fig. 2(c). When α increases from 26 to 26.3° , and further to 26.5° , the flow changes from chaotic to quasiperiodic and to period-doubling state. For $\alpha=26.3^\circ$ [Fig. 5(e)], the power spectrum exhibits a second frequency f_2 ; the subharmonic primary frequencies $f_1/2$, $f_1/4$, and $f_1/8$; and the peaks related to linear combinations $m_1(f_1/8) + m_2f_2$. It means that both the period-doubling and incommensurate bifurcations coexist in this flow system. The phase-space plot depicts two limit tori, representing that the flow behavior is dominated by the quasiperiodic state. Then, at $\alpha=26.5^\circ$ [Fig. 5(f)], a sequence of successive period-doubling bifurcations happens in view of the subharmonic primary frequencies and eight limit cycles. When α increases further, the system dynamics at $\alpha=28$ and 30° in Figs. 5(g) and 5(h) are similar to the cases at $\alpha=24$ and 21° , respectively. We also notice that, as typically shown in Fig. 5, one period-doubling event occurs as $\alpha < 26^\circ$ approximately and several period-doubling events happen as $\alpha > 26^\circ$.

Finally, flow past an elliptic airfoil with different thickness ratios (λ) is briefly studied to examine the influence of the geometry of body on the transition process. Typical results are shown in Fig. 2(c) for $Re=600$. At $\lambda=0.1$, the transition process is similar to the flat plate flow shown in Fig. 5. As λ increases, say, $\lambda=0.3$, only the period-doubling bifurcations occur. Based on extensive results (not shown here), we find that the regions of chaotic state and various incommensurate bifurcations shrink gradually with the increase in λ .

In summary, the transition route from steady to chaotic

state for flow past an inclined flat plate has been studied. A transition process via the sequential occurrence of the period-doubling bifurcations and the various incommensurate bifurcations is revealed. The results obtained in this study complement the transition phenomenon from steady to chaotic flow.

This work was supported by the National Natural Science Foundation of China (Grants No. 10832010 and No. 90405007) and the Innovation Project of the Chinese Academy of Sciences (Grant No. KJCX2-YW-L05).

-
- [1] M. Feigenbaum, *J. Stat. Phys.* **19**, 25 (1978).
 [2] M. Feigenbaum, *J. Stat. Phys.* **21**, 669 (1979).
 [3] D. Ruelle and F. Takens, *Commun. Math. Phys.* **20**, 167 (1971).
 [4] S. Newhouse, D. Ruelle, and F. Takens, *Commun. Math. Phys.* **64**, 35 (1978).
 [5] P. Manneville and Y. Pomeau, *Physica D* **1**, 219 (1980).
 [6] M. Giglio, S. Musazzi, and U. Perini, *Phys. Rev. Lett.* **47**, 243 (1981).
 [7] Ch. Jung, B. Huke, and M. Lücke, *Phys. Rev. Lett.* **81**, 3651 (1998).
 [8] J. B. McLaughlin and S. A. Orszag, *J. Fluid Mech.* **122**, 123 (1982).
 [9] A. M. Guzmán and C. H. Amon, *J. Fluid Mech.* **321**, 25 (1996).
 [10] D. Molenaar, H. J. H. Clercx, and G. J. F. van Heijst, *Phys. Rev. Lett.* **95**, 104503 (2005).
 [11] C. P. Jackson, *J. Fluid Mech.* **182**, 23 (1987).
 [12] G. E. Karniadakis and G. S. Triantafyllou, *J. Fluid Mech.* **238**, 1 (1992).
 [13] D. Yu, R. Mei, and W. Shyy, *Int. J. Numer. Methods Fluids* **39**, 99 (2002).
 [14] Y. Peng, C. Shu, Y. T. Chew, X. D. Niu, and X.-Y. Lu, *J. Comput. Phys.* **218**, 460 (2006).
 [15] P. Lallemand and L. S. Luo, *J. Comput. Phys.* **184**, 406 (2003).
 [16] T. Gao, Y.-H. Tseng, and X.-Y. Lu, *Int. J. Numer. Methods Fluids* **55**, 1189 (2007).
 [17] T. Gao and X.-Y. Lu, *Phys. Fluids* **20**, 087101 (2008).
 [18] P. Brancher and J. M. Chomaz, *Phys. Rev. Lett.* **78**, 658 (1997).
 [19] E. Ott, *Chaos in Dynamical Systems* (Cambridge University Press, Cambridge, U.K., 2002).
 [20] C. H. K. Williamson and R. Govardhan, *Annu. Rev. Fluid Mech.* **36**, 413 (2004).
 [21] M. T. Rosenstein, J. J. Collins, and C. J. De Luca, *Physica D* **65**, 117 (1993).